Journal of Electroanalytical Chemistry 755 (2015) 136–142

Contents lists available at ScienceDirect

Journal of Electroanalytical Chemistry

journal homepage: www.elsevier.com/locate/jeac

Diffusional impacts of nanoparticles on microdisc and microwire electrodes: The limit of detection and first passage statistics

Shaltiel Eloul, Enno Kätelhön, Christopher Batchelor-McAuley, Kristina Tschulik, Richard G. Compton *

Department of Chemistry, Physical and Theoretical Chemistry Laboratory, South Parks Road, Oxford University, Oxford OX1 3QZ, United Kingdom

ARTICLE INFO

Article history:
Received 19 June 2015
Received in revised form 24 July 2015
Accepted 25 July 2015
Available online 4 August 2015

Keywords:
Microdisc
Microcylinder
Wire electrode
Microwire electrode
Nanoparticle detection
Nanoparticle voltammetry
Ultra-low concentration
Nano-impacts

ABSTRACT

We derive approximate expressions for the average number of diffusive impacts/hits of nanoparticles on microdisc and microwire electrodes for the case where the impact leads to the loss of the nanoparticles from solution either via irreversible adsorption or complete electro-dissolution. The theory can also be applied to submicrometre size electrodes (nano-electrodes). The resulting equations can be utilised to analyse the number of impacts and its variance in the 'nano-impact' experiment. We also provide analytical expressions for the first passage time of an impact for dilute nanoparticle solutions in the continuum limit of Fickian diffusion. The expressions for the first passage times are used to estimate the lower limit of detection in ultra-dilute nanoparticle solutions for typical nano-impact experiments, and show the advantage of using microwire electrodes in ultra-dilute solutions or solutions containing larger nano-particles.

1. Introduction

Since nanoparticles are commonly used in many industrial and research applications, there is a strong demand for fast and cost-efficient characterisation methods on the respective particle's size and shape which are crucial requirements for understanding their physiochemical function in nanomaterials and, hence, for further developments in this field [1,2]. Alongside this, there is a growing interest in efficient ways to track and detect the large scale release of nanoparticles into the environment, especially in the light of rising concerns regarding the possible toxicity of various nano-sized particles [3,4].

The electrochemical detection of nanomaterials via the 'nano-impact' method offers significant advantages over conventional optical techniques, including the ability to analyse nanoparticles in-situ without the need for drying or modifying the investigated solution [5,6]. In the 'nano-impact' method, nanoparticles diffuse freely in an electrochemical cell, and are detected via their stochastic hits on an electrode, which may also be referred to as an 'impact'. Typically, micrometre sized electrodes are used to avoid large capacitance noise [7,8] or simultaneous impacts. During an impact event, the impacting particle may be involved in an electrochemical reaction at the electrode surface, which may result in a direct oxidation of the nanoparticle itself, while a corresponding current is measured [9–11]. Characteristics of the peak provide direct information about the individual nano-particle size, and the average number of impacts as a function of time can be described by Fick's diffusion equation, providing a practical way to measure the concentration of nanoparticles in a sample. Another possible reaction mechanism are mediated reactions, where, during the time of contact, an electrochemical reaction on the surface of the temporarily-biassed nanoparticle is enabled and recorded. This allows for the investigation of the electrocatalytic activity of the particle [6,12] and delivers information on the nanoparticle's Brownian motion at the electrode surface [13,14]. The nano-impact method has been used to identify various types of nanoparticles [15,5,10,16,17], and to provide fundamental insights into chemical mechanisms [18–22], agglomerations and aggregations [23,24], and the sensing at low nanoparticle concentrations for environmental studies [10].

Recently, we have derived probability expressions using Fick's second law to predict the number of diffusional impacts of nanoparticles that are fully dissolved on spherical and planar electrodes [25]. It was also shown how the variance of the probability expressions behaves in the Poisson limit [25]. Furthermore, analytical expressions were derived for the average first passage time as an indication of the lower concentration limit of detection. Having reported in depth the comparison between the radial and linear diffusion regime for the case of spherical and planar electrodes, in the present paper we adapt this method to microdisc and microcylinder geometries, as the importance of such electrodes for nano-impacts is enormous: The use

* Corresponding author.
E-mail address: richard.compton@chem.ox.ac.uk (R.G. Compton).

http://dx.doi.org/10.1016/j.jelechem.2015.07.042
1572-6657/

of microdisc electrodes is the common way of measuring impacts in the radial diffusion regime [10,5,11,15], and by utilising microwire (microcylinder) electrodes the detection of nano-particles in the femto-molar concentration region is enabled [26]. This study is focused on impacts which lead to the loss of the nanoparticles from solution, either via irreversible adsorption or electro-dissolution. This assumption allows us to investigate the case of diffusion towards a fully absorbing wall [25].

2. Theory

This study is divided into the cases of (*i*) microdisc and (*ii*) microwire electrodes. In both cases we start with solutions of Fick's diffusion equation:

$$\frac{\partial c}{\partial t} = D\nabla^2 c \tag{1}$$

where c is the concentration and D is the diffusion coefficient of the nanoparticles. Previously known analytical expressions, which are approximate solutions for the mass transport in chronoamperometry, are employed as a starting point.

2.1. Microdisc electrode

We assume a diffusion controlled process of independent particles in a cell that contains a microdisc electrode. In cylindrical coordinates the diffusion equation is given by:

$$\frac{\partial c(r,z,t)}{\partial t} = D\left(\frac{\partial^2 c(r,z,t)}{\partial r^2} + \frac{\partial^2 c(r,z,t)}{\partial z^2} + \frac{1}{r}\frac{\partial c(r,z,t)}{\partial r}\right). \tag{2}$$

Since the considered system features symmetry with respect to the z-axis, we can neglect the angular terms of the Laplacian. Further assuming destructive impacts, the boundary conditions are given by a fully absorbing surface, where the concentration $c(r,0,t) = 0$, on the electrode surface and $\partial c/\partial z = 0$ at all other boundaries. Far from the electrode, at $z, r \to \infty$, we set the bulk concentration $c = c^*$ at any time and the concentration in all spaces is also set to c^* at $t = 0$. Saito found the steady state flux towards a disc electrode under such conditions to be [27]:

$$J(t\to\infty) = 4Dc^* r_d \tag{3}$$

where r_d is the disc radius. An approximate solution valid for all time is given by the Shoup and Szabo equation [28]:

$$J = 4Dc^* r_d f(\tau) \tag{4}$$

where

$$f(\tau) = 0.7854 + 0.8862\tau^{-1/2} + 0.2146\exp\left(-0.7823\tau^{-1/2}\right) \tag{5}$$

and τ is a dimensionless time parameter, which is defined as:

$$\tau = 4Dt/r_d^2. \tag{6}$$

This convenient expression is widely used and provides accuracy within 0.6% compared to simulations by Heinze [29]. Via a previously discussed approach [25], we utilise this solution to study the probability of finding $\hat{N}_{hits}(t)$ (we use the term 'hits' in the symbol for consistency with previous work [25], but in the text we refer to 'hit' as an 'impact') within the time t after the experiment was started. In particular, we replace the concentration with the probability density (p^*) of finding a particle at t_0 at a given position and the flux with the accumulated number of impacts ($\hat{N}_{hits}(t)$) in a dilute solution:

$$J = \frac{d\hat{N}_{hits}(t)}{dt} = 4Dp^* r_d f(\tau). \tag{7}$$

Integrating over time gives the accumulated number of impacts:

$$\hat{N}_{hits}(t) = \int_0^t 4Dp^* r_d f(\tau)dt. \tag{8}$$

In order to solve this equation, we transform the integration variable t to τ:

$$\hat{N}_{hits}(t) = \int_0^\tau p^* r_d^3 f(\tau)d\tau. \tag{9}$$

The integration of the Shoup–Szabo equation can be calculated via a power series expansion of the exponential term:

$$\begin{aligned}&\beta\exp\left(-\alpha\tau^{-1/2}\right)\\ &= \beta\left(1-\alpha\tau^{-1/2} + \frac{\alpha^2}{2!}\tau^{-1} - \frac{\alpha^3}{3!}\tau^{-3/2} + \ldots + \frac{(-\alpha)^n}{n!}\tau^{-n/2}\right).\end{aligned} \tag{10}$$

Integration then gives:

$$\hat{N}_{hits}(t) = p^* r_d^3 F(\tau) \tag{11}$$

where:

$$\begin{aligned}F(\tau) &= \tau + 1.437\sqrt{\tau} + 6.567\cdot 10^{-2}\ln\tau\\ &\quad + \frac{3.425\cdot 10^{-2}}{\sqrt{\tau}} - \frac{3.349\cdot 10^{-3}}{\tau}\end{aligned} \tag{12}$$

when taking into account the first five terms. This expression was already derived and is used for determining concentration in the 'nano-impact' experiment [10]. Under common experimental conditions, $\tau \gg 0$, it is only necessary to use the first three terms of the Taylor series, as the fourth and above terms add less than 0.6% to the accuracy. Therefore, the solution for the average number of impacts is:

$$\hat{N}_{hits}(t) = p^* r_d^3\left(\tau + 1.437\sqrt{\tau} + 6.567\cdot 10^{-2}\ln\tau\right),\ \tau = 4Dt/r_d^2. \tag{13}$$

The average first passage time can then be found by solving $\hat{N}_{hits}(t) = 1$:

$$\frac{1}{p^* r_d^3} = \tau + 1.437\sqrt{\tau} + 6.567\cdot 10^{-2}\ln\tau. \tag{14}$$

Boika and Bard recently suggested an approach to finding the first passage time of impacts on a microdisc electrode [30] and predict an inverse proportionality between the number of impacts and the nanoparticle concentration. The above analytical solution agrees with this finding under certain experimental conditions: At large τ, i.e. $\tau \gg 100$, Eq. (14) can be simplified to an inverse linear relation of concentration with time:

$$\frac{1}{4Dp^* r_d} = t. \tag{15}$$

If we, however, calculate τ for a typical nanoimpact experiment using a microdisc electrode of the radius 5 μm and a particle concentration of 5 pM, the average first passage time is found to be $\tau = 1.12$ using the approach presented here, while neglecting the non-linear terms in Eq. (14) leads to a value of $\tau = 2.65$, which deviates by more than 100%. The dependency of the first passage time on concentration is detailed later in the Discussion section.

Moreover, we suggest the use of the first passage time as a practical indication for the lower limit of detection in terms of the nanoparticle concentration but not a suitable method for measuring nanoparticles directly. The duration of 'nano-impact' experiments is limited for experimental reasons [31], thus the first passage time provides an indication for the overall time needed to conduct an experiment. We previously [25] showed that the variance of the number of impacts detected in an experiment can be modelled in the Poisson limit. This means that the standard deviation (SD) follows the square root of the expected number of impacts and the standard deviation of one hit is hence 100%. Therefore, the duration of an experiment must be significantly longer than the expected first passage time.

2.2. Microwire electrode

Szabo [32] found an expression for the transient flux towards a semi-infinite hemicylinder, which is accurate to within 1.3% for short and long times:

$$J(t) = \pi D c^* l f(\tau) \tag{16}$$

where l is the length of the cylinder and $f(\tau)$ is:

$$f(\tau) = \frac{e^{-\sqrt{\pi\tau}/10}}{\sqrt{\pi\tau}} + \frac{1}{\ln\left[(4e^{-\gamma}\tau)^{1/2} + e^{5/3}\right]}. \tag{17}$$

τ is defined as $Dt/{r_c}^2$, where r_c is the radius of the cylinder, and $\gamma = 0.5772$ is the Euler–Mascheroni constant. Again, we integrate over time to find the average number of impacts on a cylinder (twice the surface of a hemi-cylinder):

$$\hat{N}_{hits}(t) = \int_0^t 2\pi D p^* l f(\tau) dt = \pi D p^* l \int_0^t \frac{e^{-\sqrt{\pi\tau}/10}}{\sqrt{\pi\tau}} + \frac{1}{\ln\left[(4e^{-\gamma}\tau)^{1/2} + e^{5/3}\right]} dt. \tag{18}$$

Changing the variable t to τ we obtain:

$$\hat{N}_{hits}(t) = \int_0^\tau 2\pi p^* l r_c^2 f(\tau) d\tau. \tag{19}$$

The integration of the Szabo equation can be solved as follows. The integral of the first term can be found by substituting $-\sqrt{\pi\tau}/10 = x$:

$$\int_0^\tau \frac{e^{-\sqrt{\pi\tau}/10}}{\sqrt{\pi\tau}} d\tau = -20\frac{e^{-\sqrt{\pi\tau}/10}}{\pi}\Big|_0^\tau. \tag{20}$$

The second term has the form:

$$\frac{1}{\ln\left[(4e^{-\gamma}\tau)^{1/2} + e^{5/3}\right]} d\tau = \frac{1}{\ln\left[\alpha\tau^{1/2} + \beta\right]} d\tau \tag{21}$$

where $\alpha = 2e^{-\gamma/2}$ and $\beta = e^{5/3}$. By substitution of $\alpha\tau^{1/2} + \beta = e^x$ we obtain:

$$\tau = \frac{(e^x - \beta)^2}{\alpha^2},\ d\tau = \frac{2e^x(e^x - \beta)}{\alpha^2} dx. \tag{22}$$

Substitution in Eq. (21) yields:

$$\int_0^\tau \frac{1}{\ln\left[\alpha\tau^{1/2} + \beta\right]} d\tau = \int_{\ln(\beta)}^{\ln\left(\alpha\tau^{1/2}+\beta\right)} \frac{2}{\alpha^2}\frac{e^x(e^x - \beta)}{x} dx = \frac{2}{\alpha^2}(Ei(2x) - \beta Ei(x))\Big|_{\ln(\beta)}^{\ln\left(\alpha\tau^{1/2}+\beta\right)} \tag{23}$$

where $Ei(x)$ is the exponential integral:

$$Ei(x) = \int_{-x}^{\infty} \frac{e^x}{x} dx = \gamma + \ln(x) + \sum_{k=1}^{\infty} \frac{x^k}{k \cdot k!}. \tag{24}$$

The integration of $F(\tau)$ then gives:

$$F(\tau) = \frac{\hat{N}_{hits}(t)}{2\pi p^* l r_c^2} = \int_{\tau_0}^{\tau} f(\tau) d\tau = -20\frac{e^{-\sqrt{\pi\tau}/10}}{\pi} + \frac{2}{\alpha^2}(Ei(2x[\tau,\tau_0]) - \beta Ei(x[\tau,\tau_0])) \tag{25}$$

and substituting the Ei (exponential integral), we find:

$$F(\tau) = 11.69 - 20\frac{e^{-\sqrt{\pi\tau}/10}}{\pi} + \frac{2(1-\beta)}{\alpha^2}\ln x + \frac{2}{\alpha^2}\sum_{k=1}^{\infty}\frac{\left(2^k - \beta\right)[\ln x]^k}{k \cdot k!} \tag{26}$$

where

$$x = \ln\left(\alpha\tau^{1/2} + \beta\right),\ \alpha = 2e^{-\gamma/2},\ \beta = e^{5/3}, \gamma = 0.5772. \tag{27}$$

The numerical integration of $f(\tau)$ and the approximate expression for $F(\tau)$ (Eq. (26)) are compared in Fig. 1. The figure shows that in order to reach good accuracy in the range $\tau = 0$ to 1000 many terms are needed, which makes this expression impractical.

Therefore as a practical alternative we propose a fit for the numerical integration of $f(\tau)$, from within the range from $\tau_0 = 0$ to $\tau = 1000$:

$$F^*_{short}(\tau<1000) = 0.60\tau - 20\frac{e^{-\sqrt{\pi\tau}/10}}{\pi} - 0.1591\tau^{1.1} - 3.5e^{-0.02\tau} + 9.866. \tag{28}$$

This expression is in good agreement with the numerical integration of Szabo's equation. The numerical integration was solved in Matlab by using quadratic adaptive integration with an absolute error tolerance of 10^{-10} and a relative error tolerance of 10^{-6}. Fig. 2 shows the agreement between the numerical integration of Shoup's equation and $F^*(\tau)$ in the considered range of $0 < \tau < 1000$.

However for sub-micrometre sized electrodes and nano-electrodes τ can easily exceed 1000 in a typical experiment. Therefore, we also fit Szabo's integration to another function in the range $\tau \geq 1000$:

$$F^*_{long}(\tau \geq 1000) = 292.2 + \frac{2.03(\tau - 1000)}{\ln(\tau)} - 0.7\sqrt{\tau - 1000}e^{-\frac{1000-\tau}{40{,}000}}. \tag{29}$$

This function was found to be accurate for $\tau \geq 1000$.[1]

The final expression for the average number of impacts on a cylinder is hence given by:

$$\hat{N}_{hits}(t) = 2\pi p^* l r_c^2 F^*(\tau),\ \tau = Dt/r_c^2 \tag{30}$$

where p^* is the particle number concentration, l is the length of the cylinder and r_c is the cylinder radius. The standard deviation follows $\sqrt{\hat{N}_{hits}(t)}$ and the average first passage time can be calculated by choosing $\hat{N}_{hits}(t) = 1$. $F^*(\tau)$ is defined through Eqs. (28) and (29) for the ranges $0 < \tau < 1000$ and $\tau \geq 1000$, respectively.

3. Discussion

In this section, we present a parameter study by applying the above calculated expressions for the average number of impacts in a given

[1] The agreement with the numerical integration method used is better than 1% for all τ, except for $0.1 < \tau < 12$ where the error can be up to 2.4%.

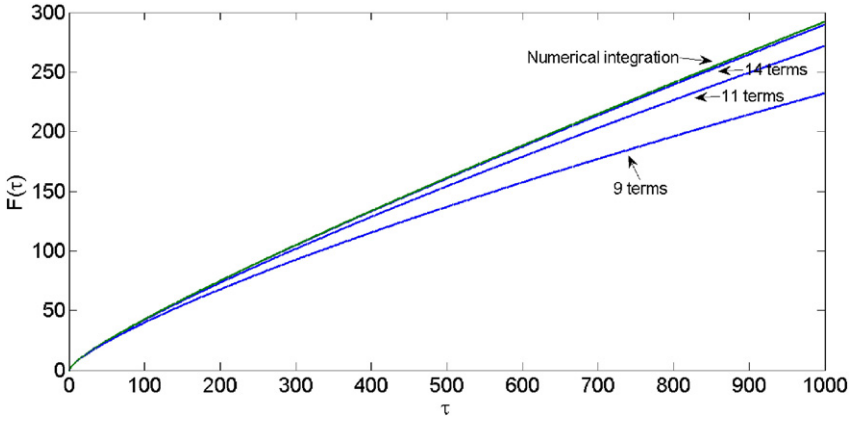

Fig. 1. Comparison between the numerical integration of Shoup's $f(\tau)$ and the analytically found expression using the first terms of the infinite sum.

time in the 'nano-impact' experiment. The results are divided into the case of a microdisc electrode and the case of a wire electrode. Additionally, first passage times are discussed as functions of the electrode size and nanoparticle the concentration.

3.1. Microdisc electrode

The number of impacts was calculated for a representative electrochemical cell containing a microdisc electrode, a nanoparticle concentration of $c^* = 1$ pM, and diffusion coefficient of 10^{-10}m^2 s^{-1}. Plots of the average number of impacts as a function of time are shown in Fig. 3 for various disc radii. It can be seen that within a typical duration of an experiment (100 s), a linear increase in the number of impacts is observed for sufficiently small radii electrode (~1 μm and below) due to the radial diffusion regime, and the expression for the number of impacts can be reduced to:

$$\hat{N}_{hits}(t) = 4Dp^* r_d t. \tag{31}$$

However, in the case of a larger radius $r_d = 10$ μm, the transient behaviour is slightly visible. The same trend can be seen as a function of the particle diffusion coefficient as shown in Fig. 4 for a 1 μm disc electrode. Since the particle size is inversely proportional to the diffusion coefficient (as described by the Stokes–Einstein equation [33]), the number of impacts gradually decreases with the particle size. For instance, at $D = 10^{-10}$ m^2 s^{-1}, which corresponds to a particle radius of ~2 nm in water, many impacts are predicted. On the other hand, particles featuring sizes larger than ~100 nm are likely to exhibit few or no impacts during the 100 s test period. It is noted, that a convergent diffusion regime which results in linear increase of the number of impacts with time is valid when $4\,Dt/r^2 \gg 1000$ according to Eq. (14). However, the first event is likely to happen also in the transient limit even at the sub-pM region, as we show next.

Fig. 5 shows an estimation of the lower limit of detection on the basis of the first passage time. We plot the first passage time as a function of the initial concentration and indicate areas, in which the standard deviation (SD) exceeds the expected number of impacts. The graphs in Fig. 5 indicate the lowest concentration that can be detected for a given size of a microdisc and a given diffusion coefficient. For example, in Fig. 5a, in the case of an electrode featuring a radius of 1 μm and a diffusion coefficient of $D = 10^{-10}$ m^2/s, the first impact occurs on average after 50 s for concentrations below 0.1 pM. Fig. 5b shows that the limit of detection can be improved by enlarging the electrode surface. Both Fig. 5a and b shows the non-linearity behaviour of the first passage time with concentration in the pM and sub-pM regions. However, inside the fM region a linear relation can be assumed as found by Boika and Bard [30].

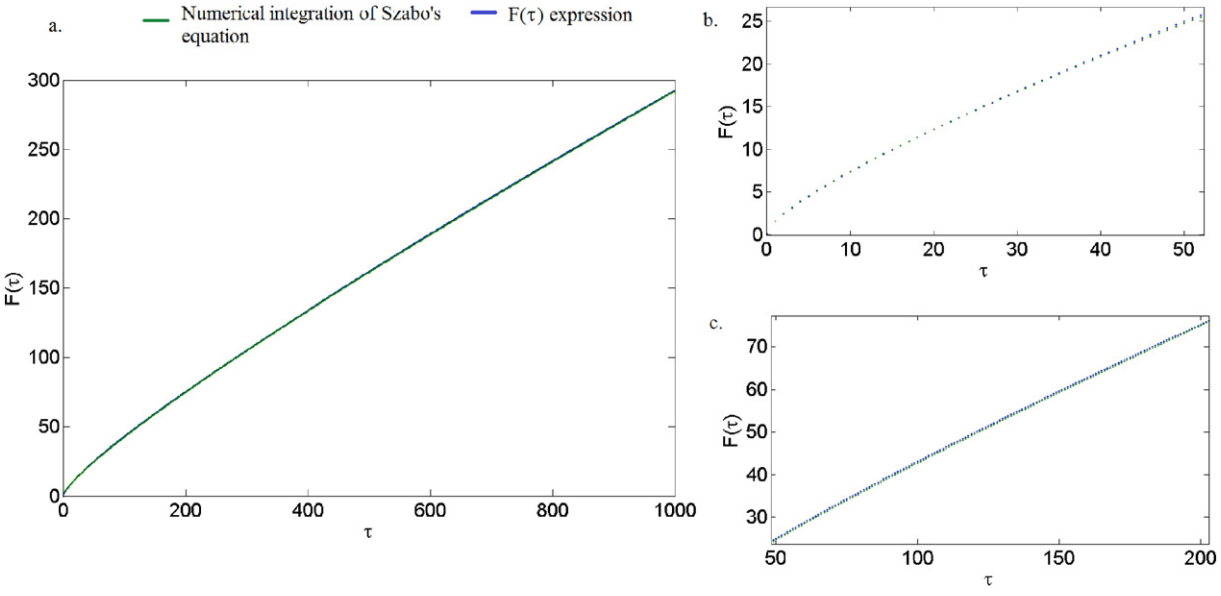

Fig. 2. Comparison between the numerical integration of Shoup's $f(\tau)$ and the suggested $F^*(\tau)$. Two sections of the graphs are exemplarily amplified in the plots b) and c).

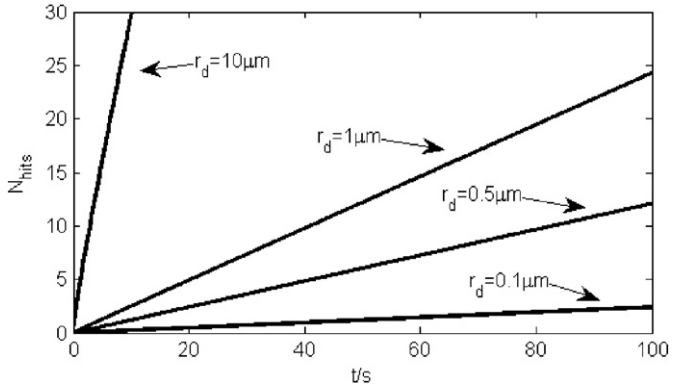

Fig. 3. Average number of impacts on a microdisc calculated for various electrode radii. The nanoparticle concentration and the diffusion coefficient are $c^* = 1$ pM and 10^{-10} m^2 s^{-1}, respectively.

3.2. Microwire electrode

A microwire (microcylinder) electrode features a macro dimension in terms of its length l and a micro dimension in terms of its radius r_c. The relation between the exposed length and the number of detected impacts is linear and can hence be utilised to adjust the sensitivity in the case of small concentrations by simply increasing the exposed length.

In Figs. 6 and 7, the number of impacts on a wire ($l = 1$ *mm*) as a function of time is plotted for various radii and various diffusion coefficients, respectively. The large number of impacts within 100 s at a concentration of 1 pM indicates the system's ability to detect nanoparticles even at ultra low concentrations, in the fM-region. It is also shown that the number of impacts gradually increases due to the large contribution of the convergent diffusion within 100 s of the experiment. For larger wire radii a non-linearity is observed, which can be understood through considering the significant contribution of the macro-size diffusion layer that is established within the first seconds of the experiment. At small radii (0.5–1 μm), however, the accumulated number of impacts is almost linear within 100 s of the experiment. Moreover, from the plots for various diffusion coefficients in Fig. 7, it can be seen that the microwire geometry exhibits good sensitivity in the detection of particle sizes larger than ~200 nm in water.

The lower limit of detection of a microwire electrode can be discussed in terms of the first passage time. The first passage time as a function of the concentration for various radii are plotted in Fig. 8. The results show the possibility of observing a large number of impacts even at ultra low concentrations sub fM regions. As the microwire geometry provides a mixed behaviour between the transient- and the steady state regime, it is particularly useful for the 'nano-impact' method. Its geometry also allows for the avoidance of shielding effects arising from the electrode support [34,35].

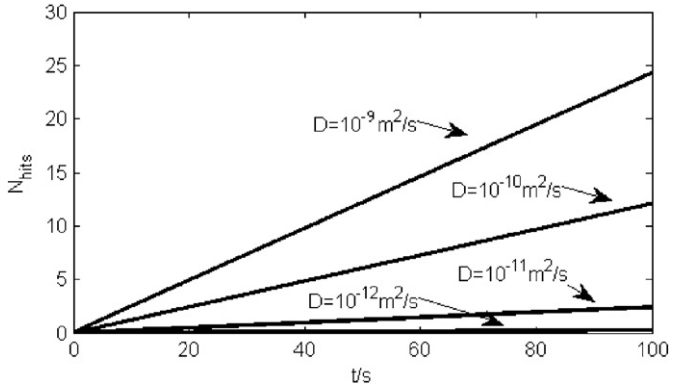

Fig. 4. Average number of impacts on a microdisc electrode featuring a radius of 1 μm in a solution of particles at a concentration of $c^* = 1$ pM for various diffusion coefficients.

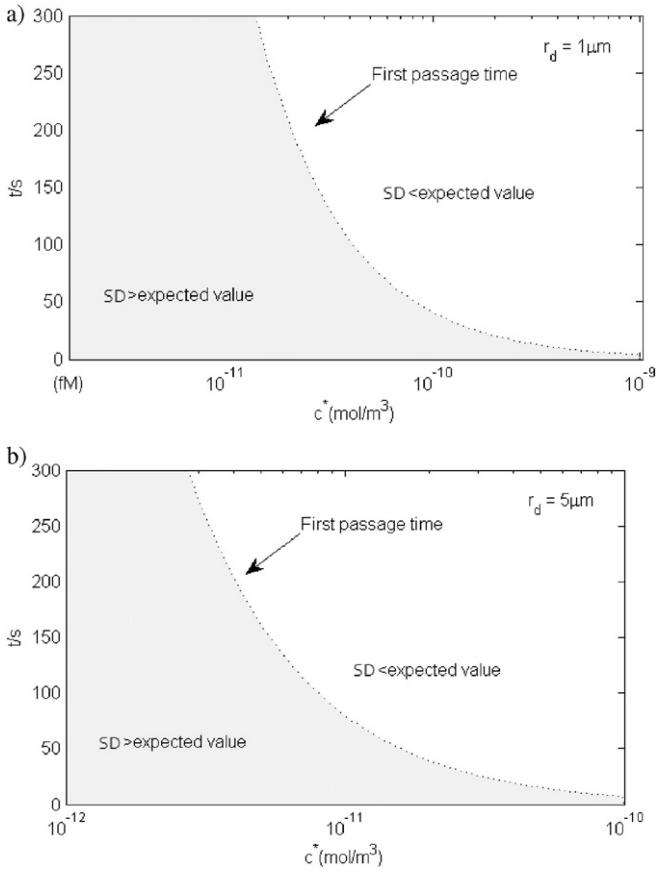

Fig. 5. The limit of detection as a function of the concentration is estimated via the first passage time for a radius of $r_d = 1$ μm (a) and $r_d = 4$ μm (b). The areas in which the standard deviation (SD) is larger than the expected value are coloured grey.

3.3. Comparison between microdisc and microwire geometries

Comparing the previous two sections, we find that there are significant advantages arising from the use of microwire electrodes over the use of microdisc electrodes. As the average number of expected impacts

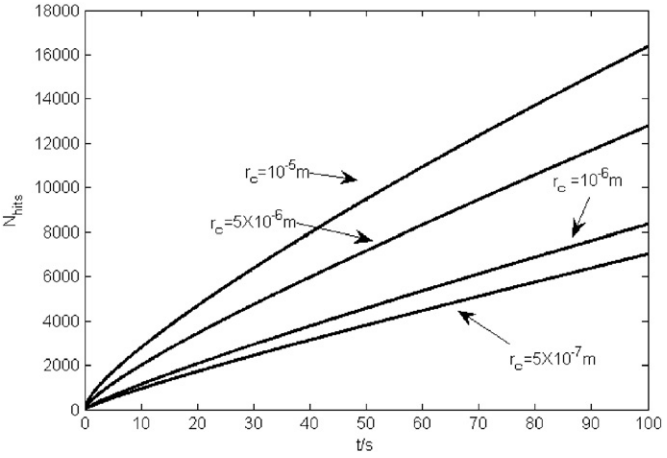

Fig. 6. Average number of impacts on a microwire electrode at various cylinder radii. The calculation employs the following parameters: $c^* = 1$ pM, l = 1 mm and D = 10^{-10} m^2 s^{-1}.

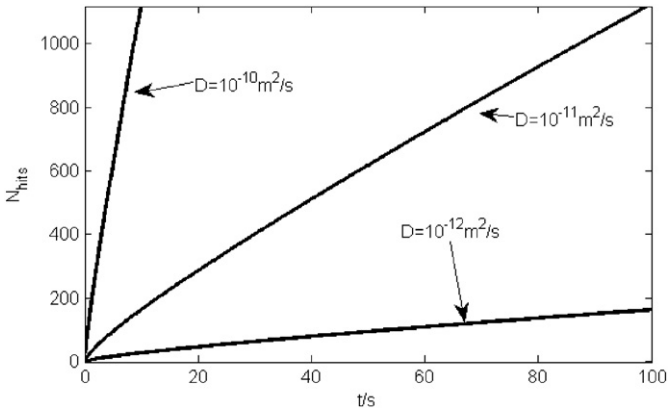

Fig. 7. Average number of impacts on a microwire electrode at a concentration of $c^* =$ 1 pM and various diffusion coefficients. The length of the wire is set to $l = 1$ mm and the wire's radius is set to $r_c = 1$ μm.

in a given time interval is proportional to a microdisc's electrode radius as well as to a wire-electrode's length, the sensitivity of both systems can be adjusted via one or the other parameter (taking into account that the overall electrode area is proportional to the capacitance background noise [7,8]). However, in the case of the microdisc, the electrode area increases quadratically with the electrode radius, while the electrode area only increases linearly with the length of the microwire electrode.

In Fig. 9a–b we show the results of the first passage time as a function of the area of the cylinder and disc electrodes at ultra-dilute solutions. Fig. 9a shows the results for 10 fM solution and Fig. 9b for 1 fM. The thickness of the microwire is fixed to a representative value of 1 μm while the length (l) varies with the areas.

The significantly lower values for the microwire electrode reveal the advantage of using microwire electrodes in 'nano-impact' experiments

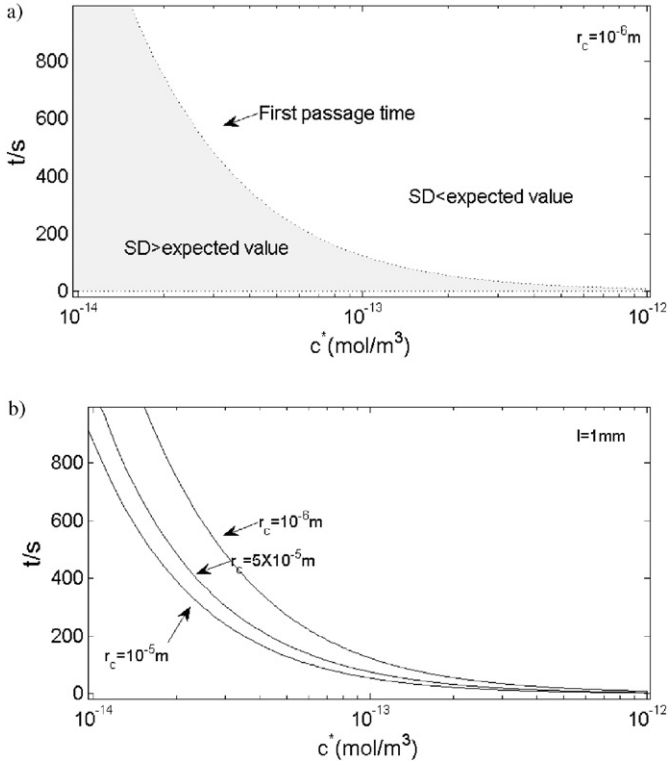

Fig. 8. a) The limit of detection as function of concentration is estimated via the first passage time for $r_c = 1$ μm and $r_d = 4$ μm. The area where the standard deviation (SD) greater than the expected value for the average number of impacts are coloured grey. b) The first passage time for various microwire radii, where l = 1 mm and D = 10^{-10} m^2/s.

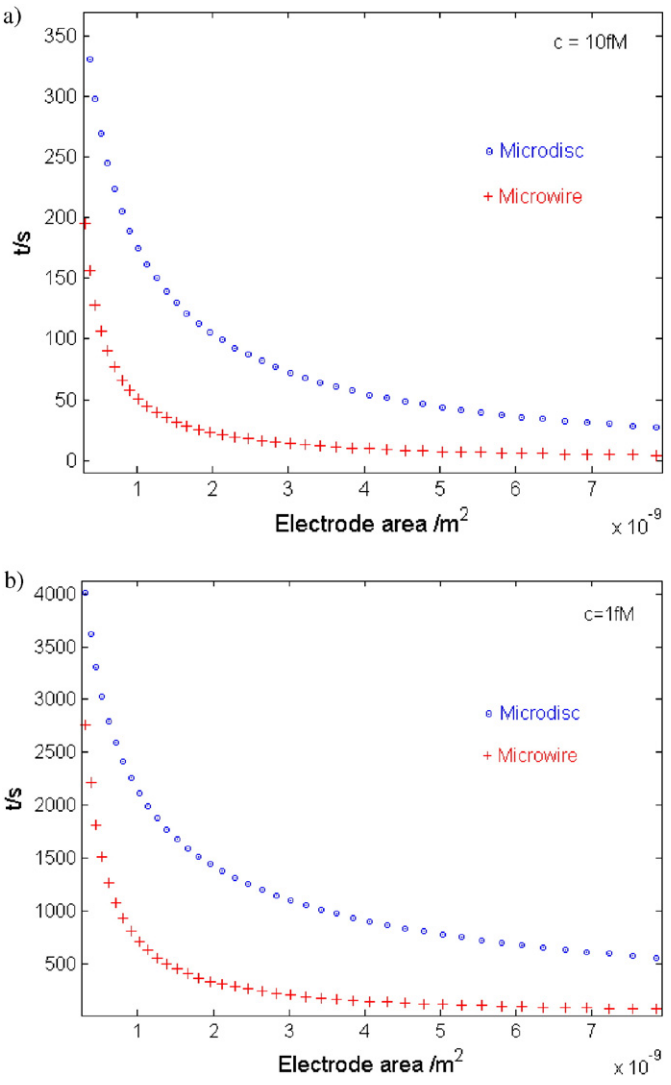

Fig. 9. Comparison of the first passage times as a function of the electrode area of a cylinder and a disc in ultra dilute solutions, 10 fM (a) and 1 fM (b). The diffusion coefficient is set to 10^{-11} m^2 $s-1$ and the thickness of the cylinder is set to 1 μm for all areas.

at ultra-low concentrations and large sizes of nano particles. Moreover, in the case of a very ultra dilute solution, 1 fM (Fig. 9b), only the microwire case shows practical values of first passage times for carrying out a 'nano-impact' experiment. For instance, if we compare a microwire electrode featuring a length of 1 mm and a radius of 1 μm with a microdisc electrode that has the same total surface area (radius of a disc set to 44.7 μm) of 6.28 nm^2 in a concentration of 1 fM and a diffusion coefficient of 10^{-11} m^2 s^{-1}, we find that the first passage time is 90 s in the microwire electrode case, and impractical value of 660 s in the microdisc electrode case, as also observed from Fig. 9b.

4. Conclusions

Analytical expressions were derived for the average number of stochastic particle impacts on microdisc- and microwire electrodes. The presented analytical expressions can be applied to 'nano-impact' experiments and provide the relation between the electrode geometry, its size, the concentration, and the number of observed impacts expected. We also provided analytical expressions for the 'first passage time', which can be used as an indication for the lower limit of detection in ultra-dilute solutions. The results for the number of hits/impacts and the first passage time in the case of microwire electrodes reveal advantages over the use of microdisc electrodes as better statistics can be

achieved even at ultra-low concentrations in the fM region while the overall electrode area and hence the capacitive background noise remains relatively small.

Acknowledgement

The research leading to these results has received funding from the European Research Council under the European Union Seventh Framework Programme (FP/2007–2013)/ERC Grant Agreement no. [320403]. KT was supported by a Marie Curie Intra European Fellowship within the 7th European Community Framework Programme Grant Agreement no. [327706].

References

[1] A. Albanese, P.S. Tang, W.C. Chan, Annu. Rev. Biomed. Eng. 14 (2012) 1–16.
[2] G. Chen, H. Qiu, P.N. Prasad, X. Chen, Chem. Rev. 114 (2014) 5161–5214.
[3] M. Ahamed, M. AlSalhi, M. Siddiqui, Clin. Chim. Acta 411 (2010) 1841–1848.
[4] N. Singh, B. Manshian, G.J. Jenkins, S.M. Griffiths, P.M. Williams, T.G. Maffeis, C.J. Wright, S.H. Doak, Biomaterials 30 (2009) 3891–3914.
[5] W. Cheng, R.G. Compton, TrAC Trends Anal. Chem. 58 (2014) 79–89.
[6] A.J. Bard, H. Zhou, S.J. Kwon, Isr. J. Chem. 50 (2010) 267–276.
[7] J. Yao, K.D. Gillis, Analyst 137 (2012) 2674–2681.
[8] C. Batchelor-McAuley, J. Ellison, K. Tschulik, P.L. Hurst, R. Boldt, R.G. Compton, Analyst 140 (2015) 5048–5054.
[9] N.V. Rees, Y.-G. Zhou, R.G. Compton, RSC Adv. 2 (2012) 379–384.
[10] E.J.E. Stuart, Y.-G. Zhou, N.V. Rees, R.G. Compton, RSC Adv. 2 (2012) 6879–6884.
[11] Y.-G. Zhou, N.V. Rees, R.G. Compton, Angew. Chem. Int. Ed. 50 (2011) 4219–4221.
[12] X. Xiao, A.J. Bard, J. Am. Chem. Soc. 129 (2007) 9610–9612.
[13] J.M. Kahk, N.V. Rees, J. Pillay, R. Tshikhudo, S. Vilakazi, R.G. Compton, Nano Today 7 (2012) 174–179.
[14] E. Kätelhön, R.G. Compton, ChemElectroChem 2 (2015) 64–67.
[15] W. Cheng, X.-F. Zhou, R.G. Compton, Angew. Chem. Int. Ed. 52 (2013) 12980–12982.
[16] L. Sepunaru, K. Tschulik, C. Batchelor-McAuley, R. Gavish, R.G. Compton, Biomater. Sci. 3 (2015) 816–820.
[17] X.-F. Zhou, W. Cheng, C. Batchelor-McAuley, K. Tschulik, R.G. Compton, Electroanalysis 26 (2014) 248–253.
[18] X.-F. Zhou, W. Cheng, R.G. Compton, Nanoscale 6 (2014) 6873–6878.
[19] T.M. Alligrant, E.G. Nettleton, R.M. Crooks, Lab Chip 13 (2013) 349–354.
[20] D. Qiu, S. Wang, Y. Zheng, Z. Deng, Nanotechnology 24 (2013) 505707 (7 pp.).
[21] K. Tschulik, W. Cheng, C. Batchelor-McAuley, S. Murphy, D. Omanović, R.G. Compton, ChemElectroChem 2 (2015) 112–118.
[22] W. Cheng, R.G. Compton, Angew. Chem. Int. Ed. 53 (2014) 13928–13930.
[23] J.C. Lees, J. Ellison, C. Batchelor-McAuley, K. Tschulik, C. Damm, D. Omanović, R.G. Compton, ChemPhysChem 14 (2013) 3895–3897.
[24] K. Tschulik, R.G. Compton, Phys. Chem. Chem. Phys. 16 (2014) 13909–13913.
[25] S. Eloul, E. Kätelhön, K. Tschulik Batchelor-McAuley, R.G. Compton, J. Phys. Chem. C (2015)http://dx.doi.org/10.1021/acs.jpcc.5b03210.
[26] J. Ellison, C. Batchelor-McAuley, K. Tschulik, R.G. Compton, Sensors Actuators B Chem. 200 (2014) 47–52.
[27] Y. Saito, Rev. Polarogr. 15 (1968) 177–187.
[28] D. Shoup, A. Szabo, J. Electroanal. Chem. Interfacial Electrochem. 140 (1982) 237–245.
[29] J. Heinze, J. Electroanal. Chem. Interfacial Electrochem. 124 (1981) 73–86.
[30] A. Boika, A.J. Bard, Anal. Chem. 87 (2015) 4341–4346.
[31] E. Kätelhön, W. Cheng, C. Batchelor-McAuley, K. Tschulik, R.G. Compton, ChemElectroChem 1 (2014) 1057–1062.
[32] A. Szabo, D.K. Cope, D.E. Tallman, P.M. Kovach, R. Wightman, J. Electroanal. Chem. Interfacial Electrochem. 217 (1987) 417–423.
[33] D.T. Gillespie, E. Seitaridou, Simple Brownian Diffusion: An Introduction to the Standard Theoretical Models, Oxford University Press, 2012.
[34] S. Eloul, R.G. Compton, ChemElectroChem 1 (2014) 917–924.
[35] J. Ellison, S. Eloul, C. Batchelor-McAuley, K. Tschulik, C. Salter, R.G. Compton, J. Electroanal. Chem. 745 (2015) 66–71.